Information Theoretical Analysis of Synaptic Communication for Nanonetworks

Hamideh Ramezani[1,2], Tooba Khan[2] and Ozgur B. Akan[1,2]

Abstract—Communication among neurons is the highly evolved and efficient nanoscale communication paradigm, hence the most promising technique for biocompatible nanonetworks. This necessitates the understanding of neuro-spike communication from information theoretical perspective to reach a reference model for nanonetworks. This would also contribute towards developing ICT-based diagnostics techniques for neuro-degenerative diseases. Thus, in this paper, we focus on the fundamental building block of neuro-spike communication, i.e., signal transmission over a synapse, to evaluate its information transfer rate. We aim to analyze a realistic synaptic communication model, which for the first time, encompasses the variation in vesicle release probability with time, synaptic geometry and the re-uptake of neurotransmitters by pre-synaptic terminal. To achieve this objective, we formulate the mutual information between input and output of the synapse. Then, since this communication paradigm has memory, we evaluate the average mutual information over multiple transmissions to find its overall capacity. We derive a closed-form expression for the capacity of the synaptic communication as well as calculate the capacity-achieving input probability distribution. Finally, we find the effects of variation in different synaptic parameters on the information capacity and prove that the diffusion process does not decrease the information a neural response carries about the stimulus in real scenario.

Index Terms—Nanonetworks, molecular communication, neuro-spike communication, information capacity, synaptic transmission.

I. INTRODUCTION

Nanonetworks, foundation of the evolving field of Internet of Bio-nano Things (IoBNT), are formed to perform the complex tasks by expanding the capabilities of single Nanomachines [1]. They have a wide range of applications, such as intelligent drug delivery, health monitoring, development of nano-robots, nano-processors and nano-memories. Since molecular communication is found in biological systems, understanding of this phenomenon is anticipated to greatly facilitate the realization of bio-inspired nanoscale communication network [2], [3].

Information transmission within intra-body nervous system, known as neuro-spike communication, is one of the most investigated natural processes to understand molecular communication [4]–[6]. This communication is performed using two phenomena, i.e., propagation of electrochemical impulses within neurons and releasing neurotransmitters across adjacent

[1]H. Ramezani and O. B. Akan are with the Internet of Everything (IoE) Group, Electrical Engineering Division, Department of Engineering, University of Cambridge, UK

[2]H. Ramezani, T. Khan and O. B. Akan are with the Next-generation and Wireless Communications Laboratory (NWCL), Department of Electrical and Electronics Engineering, Koc University, Istanbul, Turkey

Emails: hr404@cam.ac.uk, tkhan15@ku.edu.tr, oba21@cam.ac.uk

neurons. The electrochemical impulses are called action potential (AP) or spike that travel along the axon of a neuron. The transmitting neuron is termed as pre-synaptic neuron while the receiving neuron is called post-synaptic neuron as illustrated in Fig. 1. The axon of a pre-synaptic neuron branches out at the end to form connections with several post-synaptic neurons. The connection between these neurons, known as synapse, is a small gap forming a synaptic cleft between pre- and post-synaptic neurons. Arrival of a spike to the pre-synaptic terminal initiates the fusion of vesicles with the membrane. Then, the neurotransmitters stored inside the vesicle are released into the cleft, which then diffuse through the cleft and are captured by receptors present on post-synaptic terminal generating excitatory or inhibitory post-synaptic potential.

In nervous system, sensory information from outside world as well as signals from other organs are encoded into AP's, which are transmitted through a neuronal network to be processed by brain. Information theory provides a mean to estimate the transmission capacity of this complex communication network along with quantifying the reliability of the synaptic communication model [7] .

Neuro-spike communication has been studied from information theoretical perspective at different levels of complexities and for various network topologies [6], [8]–[10]. The capacity of neuro-spike communication is evaluated in [8], [11] using Hodgkin-Huxley (HH) model through numerical simulations. In [9], the information transfer rate for single-input single-output (SISO) system has been calculated under signal detection and signal estimation paradigms. Moreover, the closed-form expression for the capacity of SISO and multiple-input single-output (MISO) neuro-spike communication is derived in [6] using probabilistic model. This work is further extended in [12] to find the information rate in a SISO model with multiple synaptic terminals between two neurons. In [10], the upper bound of the capacity for a SISO synaptic communication is derived using Bernoulli distribution to model diffusion of neurotransmitters through the cleft, which ignores the synaptic geometry and the removal of residual neurotransmitters from the cleft. All the above cited studies have ignored the variability in the response due to (i) variations in vesicle release probability with time as explained in [13] and (ii) effect of synaptic geometry, diffusion of neurotransmitters and their clearance from the synaptic cleft, which would affect the mutual information, thus, capacity of the synaptic transmission. Recently, the variation in vesicle release probability is considered in [14], where it is shown that ignoring this variation causes overestimation of capacity of vesicle release
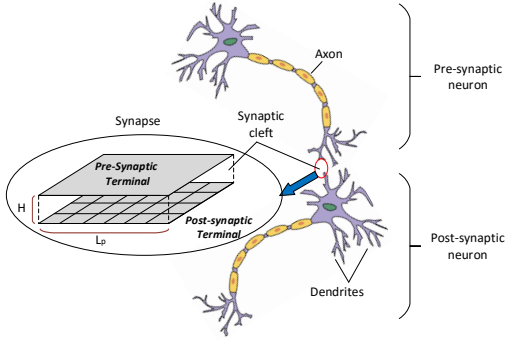
Fig. 1. Synaptic communication model.

process. Since, according to the data processing inequality, further processing does not increase the information, all of the above stated studies overestimated the capacity of the synaptic communication. Moreover, the capacity is only evaluated for the vesicle release process in [14], thus, there is a need to evaluate the capacity of complete synaptic model.

The main contribution of our paper is to derive analytical closed-form expressions for the information capacity of SISO synaptic transmission using realistic communication model for hippocampal pyramidal neurons. In our model, variation in vesicle release probability due to memory of neuron from previously released vesicles is taken into account. Moreover, the diffusion model that considers the synaptic geometry and clearance of neurotransmitters from the cleft between successive transmissions is used. Since the arrival of spike initiates the vesicle release process, the input of the system is considered as spike train. Moreover, the maximum number of bound receptors in response to each incoming spike is assumed as output since it contributes to generating the post-synaptic potential. We derive the information capacity and evaluate capacity-achieving input distribution for this SISO communication system for each incoming spike, i.e. for a single transmission. Then, to derive the overall capacity for multiple transmissions, we evaluate average mutual information using the steady-state release probability.

This whole study would serve as the basis for evaluating the capabilities of bio-inspired nanonetworks that utilize neuro-spike communication paradigm. Moreover, understanding of intra-body nervous nanonetworks from information theoretical perspective, would aid in designing ICT-inspired diagnostic and treatment techniques for neurodegenerative diseases that alter the typical ranges of the synaptic parameters. For instance, Alzheimer's disease (AD) reduces the available neurotransmitters [15], thus, decreasing the overall capacity of the synaptic transmission. Therefore, the calculation done in this paper would serve as the basis for the diagnosis of AD by comparing the capacity of healthy and diseased synapses.

The remainder of the paper is organized as follows. The synaptic communication model including vesicle release process, diffusion and receptor binding is presented in Section II. The overall capacity for multiple transmissions is derived in Section III, and numerical results are provided and analyzed
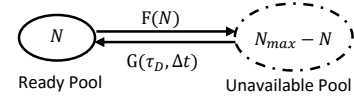

Fig. 2. Pool-based model for neurotransmitter release and replenishment.

in Section IV. Finally, the paper is concluded in Section V.

II. COMMUNICATION THEORETICAL MODELING OF SYNAPTIC TRANSMISSION

In this section, we present the communication model for three processes involved in synaptic transmission, i.e., vesicle release, diffusion and neurotransmitter-receptor binding. This communication model is later used to derive the maximum mutual information between input and output of the system.

A. Vesicle Release Process

Synaptic transmission is initiated with the arrival of spikes to the axonal terminal of the pre-synaptic neuron, which allows the influx of calcium ions by opening the voltage dependent calcium channels (VDCCs). After entering into the pre-synaptic terminal, calcium ions diffuse inside it, where they can bind to calcium buffers or sensors. Binding of enough calcium ions with a calcium sensor, which is located near the available vesicles for release, initiates the fusion of these vesicles with membrane. This causes the release of the content of vesicle, i.e., neurotransmitters, to the synaptic cleft [16].

In this paper, we consider existence of two distinct pools of vesicles in the pre-synaptic terminal as suggested in [13] and utilize the pool-based vesicle release and replenishment model shown in Fig. 2. In this model, the ready pool (RP) contains the vesicles ready for release, called readily releasable vesicles (RRVs), and the unavailable pool contains the released vesicles showing the capacity for replenishment of RP. In Fig. 2, the capacity of RP, i.e., the number of RRVs when no vesicle is released, is called N_{max}. $F(N)$ is the vesicle release probability when N, $N \leq N_{max}$, vesicles are available in RP. The mean recovery time for replenishment of one vesicle vacancy is τ_D and $G(\tau_D, \Delta t)$ is the probability of refilling one vesicle after Δt seconds.

As it is mentioned in [13], the number of vesicles that are available to refill RP is much more than N_{max}, hence, the replenishment of one released vesicle can be modeled by the first event of a Poisson process [17]. Thus, the probability of one vacancy replenishment is derived as

$$G(\tau_D, \Delta t) = 1 - \exp\left(-\tau_D^{-1} \Delta t\right) \tag{1}$$

and the number of recovered vesicles after Δt seconds is derived based on Binomial distribution given by $B(N_{\max} - N, G(\tau_D, \Delta t))$.

Vesicles can release spontaneously or upon arrival of a spike. Hence, we consider both of these scenarios while deriving the vesicle release probability.

1) Evoked Release: After arrival of a spike to the pre-synaptic terminal until release of a vesicle, the release of every RRV is independent from others. However, after release of one

vesicle, the others are temporarily prevented from release in hippocampal pyramidal neurons [13]. Hence, we utilize the uni-vesicular release model as given below.

The release probability for each of the existing vesicles in RP is governed by a Poisson process with rate $\lambda_v(t)$, which is a function of (i) opening of VDCCs and their distance from calcium sensors, (ii) binding of calcium ions to buffers, calcium sensors and pumps, and (iii) diffusion of calcium ions and buffers [18]. If a spike with duration equal to Δt_s arrives at the pre-synaptic terminal at time t_0, the vesicle release happens in the time interval given by $[t_0, t_0 + \Delta t_s]$. Thus, the fusion rate for each vesicle during a period of Δt is defined as

$$\alpha_v(\Delta t) = \int_{t_0}^{t_0+\Delta t} \lambda_v(t)dt,$$

where $\Delta t \leq \Delta t_s$. Then, as a result of using the univesicular release model, the probability of evoked release in the time interval $[t_0, t_0 + \Delta t]$ is given as [6],

$$P\{Release|Spike\ arrival\} = \begin{cases} 1 - \exp(-N\alpha_v(\Delta t)), & \Delta t \leq \Delta t_s \\ 1 - \exp(-N\alpha_v(\Delta t_s)), & \Delta t > \Delta t_s \end{cases}$$
(2)

where N is the number of RRVs.

2) Spontaneous Release: The spontaneous vesicle release is independent from evoked release. Since the average waiting time for spontaneous release of each RRV is 480 s [19], the spontaneous release probability from a synapse with N vesicles during Δt seconds is derived as follows.

$$P\{Release|No\ spike\} = 1 - \exp(-\frac{N\Delta t}{480})$$
(3)

B. Diffusion Process

After a vesicle release, neurotransmitters follow Brownian motion to diffuse across the synaptic cleft. We consider the synapse in the shape of a box with height H as shown in Fig. 1. The top and bottom surfaces of the box correspond to the pre- and post-synaptic membranes, respectively, and are considered to be infinite in dimensions. This assumption is in accordance with the diffusion model provided in [20]. After vesicle is released from pre-synaptic terminal, neurotransmitters are diffused through the cleft and captured by post-synaptic receptors present on post-synaptic density (PSD). PSD occupies a limited square shaped region on the post-synaptic terminal with side length L_p as shown in Fig. 1.

The concentration of neurotransmitters in three-dimension at any time t, denoted as $C(x, y, z, t)$, is random and its expected value can be calculated from Fick's equation given below,

$$\frac{\partial C(x, y, z, t)}{\partial t} = D_c \nabla^2 C(x, y, z, t),$$
(4)

where D_c is diffusion coefficient, $t \geq 0$ and $(x, y, z) \in \mathbb{R}^2 \times [0, H]$. While considering the reflections of neurotransmitters from pre- and post-synaptic membranes and in presence of pre-synaptic re-uptake of neurotransmitters, the solution of Fick's equation is given in [20]. This gives the expected concentration
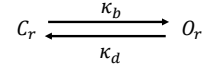
$$C_r \underset{\kappa_d}{\overset{\kappa_b}{\rightleftharpoons}} O_r$$

Fig. 3. Kinetic scheme of AMPA receptors.

of neurotransmitters in the cleft as follows,

$$C(x, y, z, t) = \frac{T_0}{(\sqrt{4\pi D_c t})^3} e^{\frac{(-x^2-y^2)}{4D_c t}}$$
$$\left\{ \sum_{k=-\infty}^{-1} (2 - P_u)(1 - P_u)^{-(k+1)} e^{\frac{-(z-(2k+1)H)^2}{4D_c t}} \right.$$
$$\left. + \sum_{k=0}^{\infty} (2 - P_u)(1 - P_u)^k e^{\frac{-(z-(2k+1)H)^2}{4D_c t}} \right\},$$
(5)

where T_0 is the number of neurotransmitters in a vesicle and P_u [uptake/hit] is the uptake probability.

On the receiver side, the neurotransmitters hit the receptors and bind to them with some probability. According to [20], we consider that receptors are uniformly distributed on the PSD and the only neurotransmitters which are inside a small volume, i.e., V_e, around each receptor are likely to bind.

To calculate the expected concentration of neurotransmitters inside V_e, i.e., C_t, we assume that there is only one neurotransmitter in the cleft. Thus, according to [20], the probability of finding that neurotransmitter inside V_e at time t is given by

$$P_e(t) = \iiint_{V_e} C(x, y, z, t)dxdydz,$$
(6)

where C is given by (5) with $T_0 = 1$.

According to [20], all particles move independently from each other. Thus, the number of neurotransmitters found inside V_e at time t can be represented by a binomial random variable, $T_e(t)$, having expected value

$$E[T_e(t)] = T_t(t)P_e(t),$$
(7)

where $T_t(t)$ is the expected total number of unbound neurotransmitters in the cleft at time t. Thus,

$$C_t \approx \frac{E[T_e(t)]}{|V_e|}$$
(8)

where $|V_e|$ is the size of the effective volume.

C. Neurotransmitter-Receptor Binding

PSD in hippocampal neurons contains two major kinds of receptors, i.e., *AMPA (α-Amino-3-hydroxy-5-methyl-4-isoxazolepropionic acid)* and *NMDA (N-methyl-D-aspartate)*. However, we only consider AMPA receptors uniformly distributed in PSD since NMDA receptors contribute in synaptic plasticity, which is not addressed in this paper. Binding of neurotransmitters to AMPA receptors increases membrane potential of post-synaptic neuron, i.e., generates excitatory post-synaptic potential (EPSP).

To derive the probability of neurotransmitter binding to an AMPA receptor, we utilize the simplified kinetic model demonstrated in Fig. 3. As it is shown in [21], this simplified
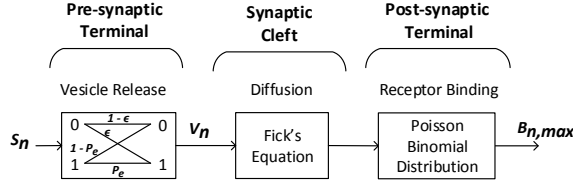
Fig. 4. Block diagram of the synaptic communication.

model provides fairly good approximations for the time course and the dynamic behavior of synaptic currents compared to the complex multi-state kinetic models.

When receptor r, $r \in [1, R_0]$, is in the closed state, i.e., C_r, it is available for binding to a neurotransmitter. After binding, the receptor moves to the open state, i.e., O_r, and allows the influx of ions that changes the membrane potential of post-synaptic terminal. The probability of being in each of these states changes with time depending on the expected concentration of neurotransmitters near receptor, i.e., C_t, as given in the following equations,

$$\frac{dC_r}{dt} = -\kappa_b C_r C_t + \kappa_d O_r,$$
$$C_r + O_r = 1, \tag{9}$$

where κ_b and κ_d are binding and dissociation rates for AMPA receptors, respectively. O_r and C_r also represent the opening and closing probabilities of AMPA receptors, respectively, that depend on both time and the position of the receptors.

III. Capacity Analysis of Synaptic Communication

The extensive analysis of synaptic transmission from information theoretical perspective is required to lay down the foundation of bio-inspired nanonetworks. Thus, in this section, we aim to derive the closed-form expression of the capacity of the synaptic transmission that depends on the availability of readily releasable vesicles, which changes with time and depends on the previous vesicle releases. Therefore, we discretize time into windows of equal durations, i.e., Δt, and select Δt sufficiently small so that at most one spike can exist at each window [6]. Note that by considering the width of spike equal to Δt_s, Δt must be selected greater than or equal to Δt_s to have complete spike duration in one window.

In each time step, we can maximize mutual information over all possible spiking probabilities to estimate capacity of the system. However, since the number of RRVs changes over time, the vesicle release probability also changes. Hence, according to the definition, mutual information would also vary with time. Thus, we need to find average mutual information from 1st to nth time step and derive the spiking probability that maximizes it to reach the overall capacity until time step n. Finally, we extend this calculation to find the capacity of synaptic transmission when n approaches to infinity.

A. Mutual Information in Each Time Step

The input and output of the synaptic communication model shown in Fig. 4 are S_n and $B_{n,max}$, respectively, in nth time

slot. Here, S_n depicts the existence of spike at input and $B_{n,max}$ shows the maximum number of bound receptors at the post-synaptic terminal as a result of vesicle release. Hence, the mutual information of the system at each time step can be defined as follows,

$$I(S_n, B_{n,max}) = \mathcal{H}(B_{n,max}) - \mathcal{H}\left(B_{n,max}|S_n\right), \tag{10}$$

where the entropies in (10) follow the general formula given as $\mathcal{H}(X_n) = -\sum_i P\{X_n = i\} \log_2 P\{X_n = i\}$.

By conditioning over the spike arrival, we can write the probability $P\{B_{n,max} = i\}$ as given below,

$$P\{B_{n,max} = i\} = \sum_{j=0}^{1} P\{B_{n,max} = i|S_n = j\}P\{S_n = j\}, \tag{11}$$

where $i \in [0, R_0]$ and R_0 is the total number of receptors on the post-synaptic terminal. Same as [6], [9], we model the spike arrival with a Poisson process. Hence, assuming the rate of this process as λ, the probability of spike arrival at nth time slot can be calculated as $P\{S_n = 1\} = 1 - exp(-\lambda \Delta t) \triangleq p$.

To derive the probability $P\{B_{n,max} = i|S_n = j\}$, we can condition over the vesicle release process as follows.

$$P\{B_{n,max} = i|S_n = j\} =$$
$$\sum_{k=0}^{1} P\{B_{n,max} = i|V_n = k\}P\{V_n = k|S_n = j\}, \tag{12}$$

where V_n indicates the release of vesicle in nth window. Since the neurotransmitters are removed from synaptic cleft between successive vesicle releases through re-uptake and diffusion [20], the synaptic noise due to residual neurotransmitters is not significant in healthy neurons and we consider $P\{B_{n,max} = 0|V_n = 0\} = 1$.

To find the probability $P\{B_{n,max} = i|V_n = 1\}$, we define the opening probability of rth receptor as $O_r(t)$, where $r \in [1, R_0]$ and $0 \leq t \leq \Delta t$. As shown in [20], a smaller time step called $\Delta \tau << \Delta t$ can be used to calculate $O_r(t)$ in each Δt. We are interested in the maximum number of bound receptors, $B_{n,max}$, since it contributes to the peak of EPSP. After binding to a neurotransmitter, the receptors stay in open state until EPSP reaches its maximum value. Hence, utilizing the maximum opening probability for rth receptor during nth time step, i.e., $O_{r,n} = \max_{0 \leq t \leq \Delta t} \left(O_r(t)\right)$, we can calculate $B_{n,max}$ by defining the variable $x_{r,n}$ as follows.

$$x_{r,n} = \begin{cases} 0, & 1 - O_{r,n} \\ 1, & O_{r,n} \end{cases}. \tag{13}$$

The $\sum_{r=1}^{R_0} x_{r,n}$ shows the maximum number of open receptors during time step Δt. Hence, the probability of having i open receptors upon vesicle release, i.e., $P\{B_{n,max} = i|V_n = 1\}$, is equal to $P\{\sum_{r=1}^{R_0} x_{r,n} = i\}$, which can be modeled by Poisson Binomial distribution with mean, μ_n, and variance, σ_n^2, as shown in [22],

$$\mu_n = \sum_{r=1}^{R_0} O_{r,n}, \tag{14}$$

$$\sigma_n^2 = \sum_{r=1}^{R_0} O_{r,n}(1 - O_{r,n}). \tag{15}$$

Thus, the probability $P\{B_{n,max} = i|V_n = 1\}$ is calculated as follows,

$$P\{B_{n,max} = i|V_n = 1\} = \frac{1}{R_0 + 1} \sum_{l=0}^{R_0} E^{-li} \prod_{r=1}^{R_0} \left[1 + (E^l - 1)O_{r,n} \right], \tag{16}$$

where $E = exp(\frac{2\sqrt{-1}\pi}{R_0+1})$.

Next step is deriving the conditional vesicle release probability given in (12), i.e., $P\{V_n = k|S_n = j\}$. As it is shown in Fig. 4, a binary channel can be used to model the vesicle release process at each time step. According to (2) and (3) and the pool-based vesicle release and replenishment model depicted in Fig. 2, the probability of release in nth time slot when RP has N vesicles is expressed as follows,

$$P\{V_n = 1|N_n = N, S_n = 1\} = 1 - \exp\left(-N\alpha_v(\Delta t_s)\right) \triangleq P_e, \tag{17}$$

$$P\{V_n = 1|N_n = N, S_n = 0\} = 1 - \exp\left(-\frac{N\Delta t}{480}\right) \triangleq \epsilon, \tag{18}$$

where (17) shows the probability of evoked release, (18) depicts the spontaneous release probability and N_n indicates the number of available vesicles in RP at the beginning of nth time slot. Then, the conditional vesicle release probability can be written as follows,

$$P\{V_n = k|S_n = j\} =$$
$$\sum_{N=0}^{N_{max}} P\{V_n = k|N_n = N, S_n = j\}P\{N_n = N\}.$$

In [14], an array named P_n is defined with dimension $1 \times (N_{\max} + 1)$ having ith element equal to $P\{N_n = i - 1\}$. Then, a recurrence relation is derived for P_n as follows,

$$P_n = P_{n-1}DR. \tag{19}$$

Here, D and R are $(N_{\max}+1) \times (N_{\max}+1)$ matrices indicating the impact of pool depletion and replenishment on the probability of having a given number of RRVs, respectively. To derive the probability of having different number of RRVs in time slot n, (19) is simplified to $P_n = P_1(DR)^{n-1}$, where P_1 is equal to $[0, 0, ..., 0, 1]$ indicating that RP is full, i.e., $N = N_{max}$, before the arrival of spikes.

The (i, j)th element of D, i.e., D_{ij}, represents the probability of transition from having $N_{n-1} = i - 1$ to $N_n = j - 1$ as a result of vesicle release. Since we are using the univesicular release model, at most one vesicle can be released from the pool. Hence, the nonzero elements of matrix D occur only where $j \in \{i, i-1\}$ and can be derived from vesicle release probability shown in Fig. 2, $F_n(.)$, as $D_{ii} = 1 - F_n(i - 1)$ and $D_{i(i-1)} = F_n(i-1)$. Using the spiking probability, p, and the probabilities given in (2) and (3), the vesicle release probability in nth slot when RP has i vesicles, i.e., $F_n(i)$, involving both spontaneous and evoked releases, is derived as follows,

$$F_n(i) = 1 - \left[\exp\left(-i\alpha_v(\Delta t_s)\right)p + \exp\left(-\frac{i\Delta t}{480}\right)(1 - p) \right]. \tag{20}$$

The (i, j)th element of R, i.e., R_{ij}, represents the probability of transition from having $N_{n-1} = i - 1$ to $N_n = j - 1$ as a result of vesicle replenishment process. Since the number of refilled vesicles when the RP has i RRVs can be derived from Binomial distribution given by $B(N_{\max} - i, G(\tau_D, \Delta t))$ as explained in Section II-A, the matrix R is an upper triangular matrix whose (i, j)th element for $\forall j \geq i$ is defined as follows,

$$R_{ij} = \binom{N_{\max} - (i - 1)}{j - i} G(\tau_D, \Delta t)^{j-i} \left(1 - G(\tau_D, \Delta t)\right)^{N_{\max}-(j-1)}.$$

B. Information Capacity of synaptic transmission

We define the maximum mutual information achieved during first n time slots as $C_n = max_p \sum_{l=1}^{n} \frac{I(S_l;B_{l,max})}{n}$. Then, the overall capacity of synaptic communication is defined as $C = \lim_{n\to\infty} C_n$, for which we evaluate the convergence of $I(S_n; B_{n,max})$. Based on the recurrent equation given by (19), the number of vesicles in RP can be modeled by a finite-state Markov chain. Moreover, the steady state probability of each state in this Markov chain, i.e., $\pi = [\pi_0, \pi_1, \ldots, \pi_{N_{\max}}]$, can be derived by solving the linear equations $\pi = \pi DR$ and $\sum_{i=0}^{N_{\max}} \pi_i = 1$. Then, to find $\lim_{n\to\infty} I(S_n; B_{n,max})$, we calculate the limit of (12) when n tends to infinity as follows,

$$\lim_{n\to\infty} P\{B_{n,max} = i|S_n = j\} =$$
$$\sum_{k=0}^{1} P\{B_{n,max} = i|V_n = k\} \sum_{N=0}^{N_{max}} P\{V_n = k|S_n = j, N_n = N\}\pi_N.$$

Now, the limit of (11) as n tends to infinity is found as

$$\lim_{n\to\infty} P\{B_{n,max} = i\} =$$
$$\sum_{j=0}^{1} P\{S_n = j\} \lim_{n\to\infty} P\{B_{n,max} = i|S_n = j\}.$$

Therefore, the mutual information, $I(S_n; V_n)$, converges as given below.

$$\lim_{n\to\infty} I(S_n; B_{n,max}) = \mathcal{H}(\lim_{n\to\infty} B_{n,max}) - \mathcal{H}(\lim_{n\to\infty} B_{n,max}|S_n)$$
$$\triangleq I_\infty, \tag{21}$$

where the entropies in the above equation follow the general formula given as

$$\mathcal{H}(\lim_{n\to\infty} X_n) = -\sum_i \lim_{n\to\infty} P\{X_n = i\} \log_2 \left(\lim_{n\to\infty} P\{X_n = i\} \right).$$

Considering the binary channel of vesicle release block in Fig. 4, since the crossover probability when there is no spike at input, ϵ, is very small in real scenario, the mutual information at the output of this block decreases if P_e reduces. Since the number of RRVs decreases with time as a result of pool depletion; according to (17), the evoked release probability, P_e, thus, $I(S_n; V_n)$, also reduces with time. Moreover, according to data processing inequality, further processing does not increase the information. Hence, $I(S_n; B_{n,max})$ also decreases with time. Furthermore, according to (21), $I(S_n; B_{n,max})$ converges to I_∞, thus, its average over time also converges to I_∞, i.e.,

$$\lim_{n\to\infty} \sum_{l=1}^{n} \frac{I(S_l; B_{l,max})}{n} = I_\infty, \tag{22}$$

TABLE I
SIMULATION PARAMETERS

Parameters	Symbols	Values
Synaptic cleft height	H	20 nm [23]
Diffusion coefficient	D_c	0.33 μm^2/ms [24]
Side length of PSD	L_p	0.4 μm [20]
Number of receptors	R_0	441 [25]
Pre-synaptic Re-uptake	P_u	10% [20]
Binding Rate of AMPA	κ_b	$78 \times 10^6 \frac{1}{\text{Ms}}$ [26]
Dissociation Rate of AMPA	κ_d	750 s^{-1} [26]
Effective Volume	V_e	$1 \times 1 \times 0.5$ nm^3
Simulation time step	$\Delta\tau$	3.85 ns [20]
Spike width	Δt_s	4 ms [16]
Discretization time step	Δt	Δt_s [14]
Average fusion rate	$\alpha_v(\Delta t_s)$	$0.06\sqrt{N}$ [27]
Mean vacancy recovery time	τ_D	$\frac{0.6}{N_{max}}$ [17]

and the capacity of synaptic communication can be calculated as follows,

$$C = \max_p I_\infty. \tag{23}$$

IV. EVALUATION

In this section, we intend to evaluate the capacity of the synaptic communication and find how it is affected by varying different synaptic parameters. Since the output of the system, i.e., the maximum number of bound receptors, depends on spiking probability, p, capacity of RP, N_{max}, and number of neurotransmitters in a vesicle, T_0, we first evaluate the impact of these parameters on the mutual information between input and output. The values of all simulation parameters are selected from the experimental studies as shown in Table I. Furthermore, we highlight how the mutual information changes over the multiple synaptic transmissions. Thus, we calculate the average mutual information over n transmissions and maximize it to find the capacity until nth time slot. Finally, with the use of steady-state probability of number of RRVs, we find the overall mutual information and capacity along with the capacity-achieving input probability distribution.

A. Mutual Information in Each Time Step

In this section, we calculate the mutual information in each time step for different values of synaptic parameters, i.e., N_{max} and T_0, and spiking probability, p, and discuss the effects of changing these parameters on information transfer rate. Since the vesicle release process is the only part of the system that has memory, i.e., the number of RRVs changes after each transmission, we analyze the impact of variation of number of RRVs with time on mutual information. Among the aforementioned parameters, T_0 is not affecting the number of RRVs, hence the average number of available vesicles for release is plotted for different values of N_{max} and p in Fig. 5.

The pool-based vesicle release and refill model shown in Fig. 2 is used to derive the statistics of number of RRVs. As it is shown in Fig. 5, the number of RRVs reduces with time, thus, we can conclude that the release rate of vesicles
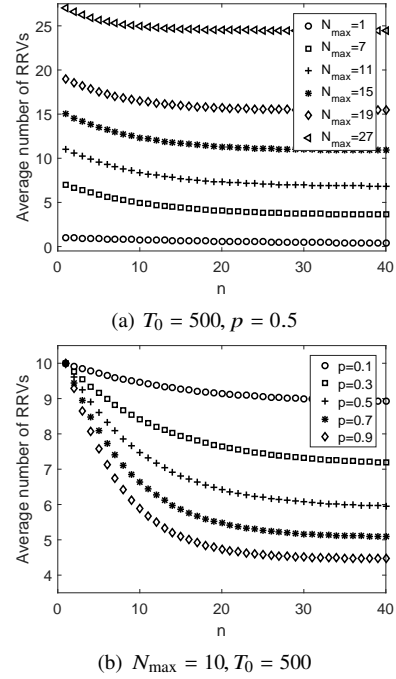

(a) $T_0 = 500$, $p = 0.5$

(b) $N_{\max} = 10$, $T_0 = 500$

Fig. 5. Average number of available vesicle for release for different (a) capacity of ready pool, N_{max} and (b) spiking probabilities, p.

is faster than their refill rate, i.e., the neuron does not have enough time between multiple transmissions to refill all of the released vesicles. It can also be observed in Fig. 5(a) that increasing N_{max} increases the average number of vesicles available in each time slot. This is due to two reasons, i.e., higher value of N_{max} results in (i) having more number of RRVs in the beginning of simulation, and (ii) faster vacancy replenishment according to the definition of τ_D given in Table I. Moreover, according to Fig. 5(b), increasing the spiking probability, p, while keeping N_{max} fixed, decreases the average number of RRVs. Since the evoked release probability, P_e, is higher than spontaneous release probability, ϵ, increasing spiking probability, p, causes the release of more number of vesicles in multiple transmissions. Moreover, the refill rate is constant, thus, the average number of RRVs decreases with time by increasing spiking probability, p.

The mutual information between input and output of the system is shown in Fig. 6 for different values of N_{max}, T_0 and p. It is observed that the mutual information reduces over time. The reason of this reduction can be explained considering the binary channel of vesicle release block in Fig. 4. Since the crossover probability when there is no spike at input, ϵ, is very small in real scenario, the mutual information at the output of this block would be maximum if $(1 - P_e)$ tends to zero, i.e., as the evoked release probability, P_e, increases. On the other hand, the diffusion and binding processes cannot increase the information about input according to the data processing inequality. Thus, the overall mutual information of the system is directly related to the evoked release probability. According to (17), this release probability decreases with reduction in the number of RRVs and the average number of RRVs reduces with time as shown in Fig. 5. Therefore, mutual information
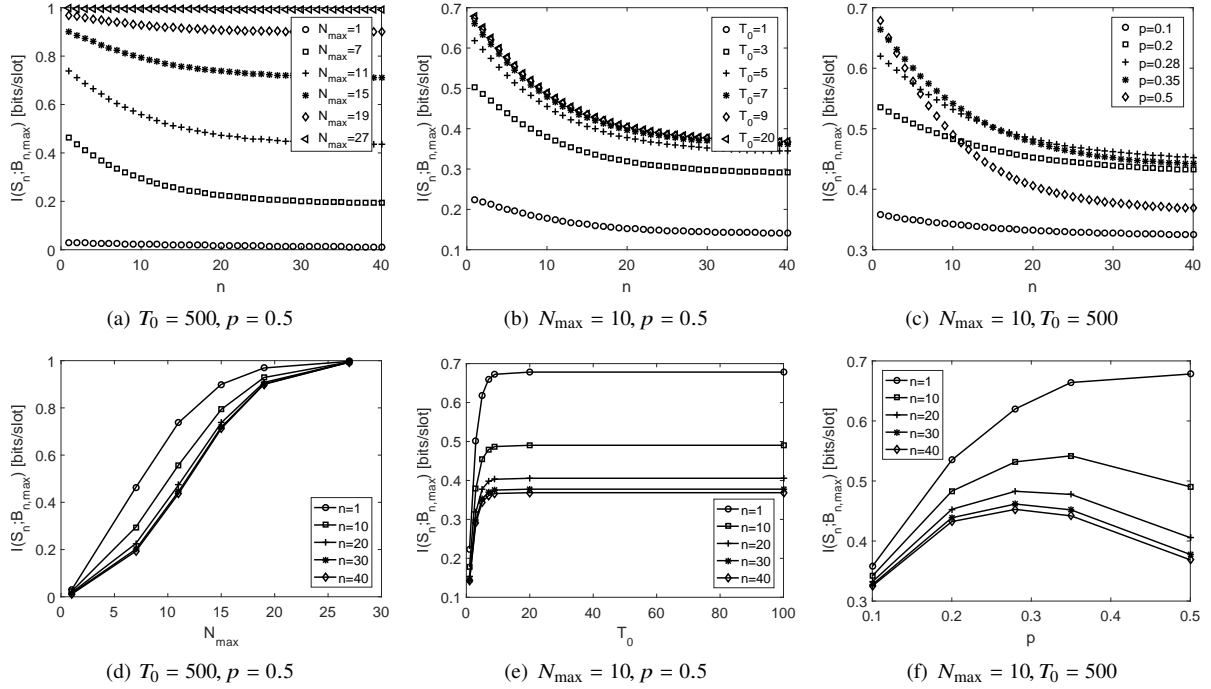
Fig. 6. Mutual information between spiking and maximum number of bound receptors for different (a,d) capacity of ready pools, N_{max}, (b,e) number of neurotransmitters in a vesicle, T_0, and (c,f) spiking probabilities, p.

also reduces over time as shown in Fig. 6. Moreover, since the number of RRVs, N_n, eventually reaches its steady state value according to the Markov chain model indicated in Section III-B, mutual information also saturates to a constant value.

In Fig. 6(a), the mutual information is plotted against time for different values of N_{max}. It can be observed that the reduction rate of mutual information decreases with the increase in the value of N_{max}. This is due the fact that high values of N_{max} leads to higher number of RRVs, N_n, in each time slot as shown in Fig. 5(a), which saturates the evoked release probability, P_e, according to (17). Therefore, the rate of change of mutual information tends to zero for higher values of N_{max} as shown in Fig. 6(a) and Fig. 6(d). Furthermore, for very low values of N_{max}, the signal transmission happens rarely, thus, mutual information is close to zero for all time.

It can also be observed in Fig. 6(a) and Fig. 6(d) that in each time slot we have higher value of mutual information as the value of N_{max} increases. This is due to having more number of RRVs, thus, higher evoked release probability, as a result of increasing N_{max}.

Next, we evaluate the effect of changing the number of neurotransmitters in a vesicle, T_0, on mutual information. We select N_{max} as 10, which is reported in [28] for average capacity of RP in hippocampal pyramidal neurons. As can be observed in Fig. 6(b) and Fig. 6(e), the output has more information about input if there is a higher number of neurotransmitters in a vesicle. Moreover, the mutual information attains saturation after certain value of T_0 as a result of having enough bound receptors to detect the signal transmission in case of spike arrival. Furthermore, for very low values of T_0, the neurotransmitters are lost in the cleft or uptaken by the pre-synaptic terminal before reaching the post-synaptic receptors,

thus, resulting in lower value of mutual information.

The change in mutual information of synaptic transmission with respect to spiking probability is shown in Fig. 6(c) and Fig. 6(f). The mutual information decreases with higher rate with increasing spiking probability as shown in Fig. 6(c). This is due to more reduction in the number of RRVs by increasing spiking probability as shown in Fig. 5(b). Moreover, since the number of RRVs, N_n, changes with time, the spiking probability that maximizes mutual information also changes in each time slot. This change is apparent in Fig. 6(f) as the peak of mutual information is moving towards left.

The mutual information between spiking and output of vesicle release process is reported in [14]. By comparing the achievable mutual information for the overall synaptic communication shown in Fig. 6 and the results of [14], we can see that the diffusion and binding processes do not decrease the mutual information after certain value of T_0. Thus, we can conclude that if the value of T_0 is very high, which is the case in real scenario [29], enough amount of the released vesicle are always received by the post-synaptic neuron, which shows the reliability of the synaptic system.

B. Average Mutual Information and Capacity for n Synaptic Transmissions

In the previous section, we observed that the mutual information changes with time, hence we need to find average mutual information over several transmissions to evaluate the capacity of synaptic communication. The mutual information averaged over n consecutive time slots, always starting from the first time slot, is shown in Fig. 7. It is apparent in the figure that average mutual information reduces as the system use increases, which is a result of the depletion of RP. Moreover,
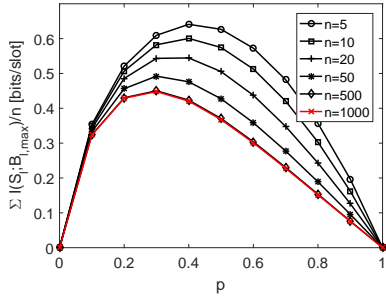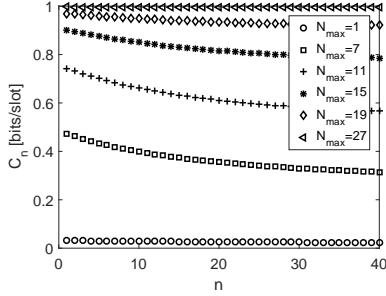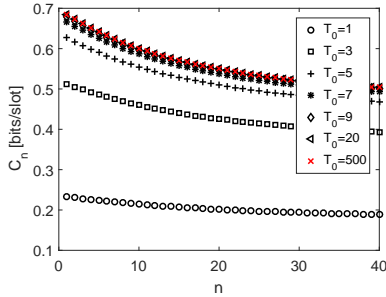
Fig. 7. Average mutual information for $N_{max} = 10$ and $T_0 = 500$.
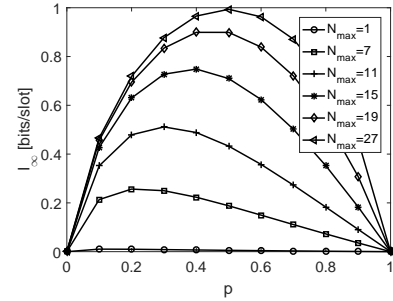

(a) $T_0 = 500$

(b) $N_{max} = 10$

Fig. 8. Maximum mutual information from 1st to nth slot for different values for (a) capacity of RP, N_{max}, and (b) number of neurotransmitters in a vesicle, T_0.

(a) $\lim_{n \to \infty} \sum_{l=1}^{n} \frac{I(S_l; V_l)}{n} = I_{\infty}$

(b) Channel capacity and optimum spiking probability

Fig. 9. Average mutual information of the system, system capacity and capacity-achieving spiking probability in steady state for $T_0 = 500$ and different values of N_{max}.

the spiking probability that maximizes the average mutual information is also decreasing with time as indicated by the peak of the curve that moves towards left.
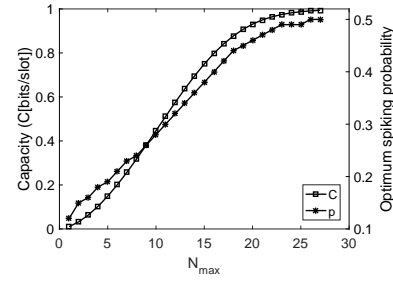
The average mutual information is maximized over spiking probability, p, to calculate the capacity over multiple transmissions, for different values of N_{max} and T_0 as shown in Fig. 8. The capacity reduces with time as a result of reduction in mutual information over multiple transmissions as observed in Fig. 6. Moreover, increase in both N_{max} and T_0 increases the capacity as a result of higher vesicle release probability and increased chances of neurotransmitters to reach the receptors, respectively. Furthermore, as we have seen in Fig. 6(e), the mutual information in each time step saturates with increasing T_0. Hence, it can be observed in Fig. 8(b) that the capacity of the system over multiple uses also saturates after a specific value of T_0.

C. Mutual Information and Capacity at Steady-State

To evaluate the capacity of synaptic communication, we calculated the steady state probabilities of having different

number of RRVs and use them to derive the mutual information between input and output of the system as n tends to infinity, I_{∞}. This also corresponds to the average mutual information evaluated over infinite consecutive time slots as given by (22).

The I_{∞} is plotted against spiking probability for different values of N_{max} and T_0 in Fig. 9(a) and Fig. 10(a), respectively. Similar to the average mutual information, we can observe that I_{∞} also increases with N_{max} and T_0. Moreover, I_{∞} is maximized over spiking probability, p, to calculate the capacity for different values of N_{max} and T_0 as shown in Fig. 9(b) and Fig. 10(b), respectively. Since changing the N_{max} affects the number of RRVs, which in turn affects the steady state probabilities of having different number of RRVs, the capacity-achieving spiking probability also changes as shown in Fig. 9. However, as it can be seen in Fig. 10, changing T_0 does not change capacity-achieving spiking probability since it is not affecting the availability of vesicles.

It can also be observed from Fig. 9(b) and Fig. 10(b) that capacity improves with increasing N_{max} and T_0, respectively. This is a result of dependence of I_{∞} on these factors as explained earlier. As it can be observed in Fig. 10(b), the capacity reaches the maximum value for T_0 around 10. However, more number of bound receptors is needed for spike generation, thus, there are more neurotransmitters in a vesicle in real scenarios. Selecting the system parameters as reported in experimental studies for hippocampal pyramidal neurons, i.e., $N_{max} = 10$ [26] and $500 \leq T_0 \leq 3000$ [29], [30], the capacity of synaptic communication model for information transmission among these neurons is calculated as $C = 0.44$ bits/slot $= 110$ bits/s. These results can be compared

(a) $\lim_{n \to \infty} \sum_{l=1}^{n} \frac{I(S_l; V_l)}{n} = I_\infty$

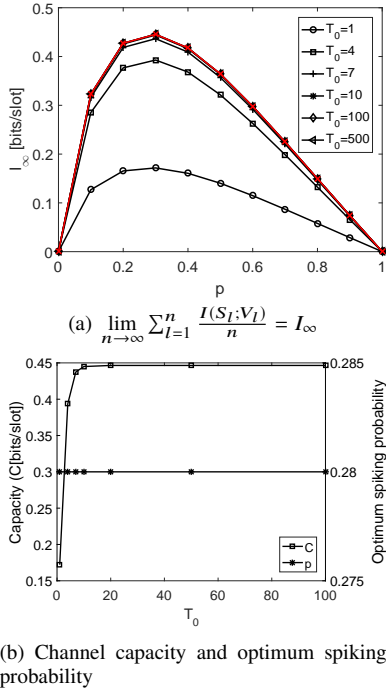(b) Channel capacity and optimum spiking probability

Fig. 10. Average mutual information of the system, system capacity and capacity-achieving spiking probability in steady state for $N_{max} = 10$ and different values of T_0.

with the results obtained from the diseased synapses to have an ICT-inspired diagnosis technique for neurodegenerative diseases. Moreover, for designing a molecular communication based nanonetworks, these results can be used to decide about the optimal parameters to achieve maximum capacity.

V. CONCLUSION

In this paper, we analyzed a realistic physical reference model as the most basic realization of nanonetworks that utilize neuro-spike communication paradigm from information theoretical perspective. We formulated the mutual information between input and output of a SISO synaptic communication for a single transmission. Since this system has memory, we found the average mutual information over multiple transmissions to evaluate its overall capacity. Moreover, we derived a closed-form expression for the capacity of synaptic transmission and calculated the capacity-achieving spiking probability. Finally, we found the effects of change in various synaptic parameters, such as spiking probability, number of readily releasable vesicles (RRVs) and number of neurotransmitters in a vesicle, on the information capacity of the system.

VI. ACKNOWLEDGMENT

REFERENCES

[1] I. F. Akyildiz *et al.*, "Nanonetworks: A new communication paradigm," *Computer Networks*, vol. 52, no. 12, pp. 2260–2279, 2008.

[2] O. B. Akan *et al.*, "Fundamentals of molecular information and communication science," *Proc. of the IEEE*, to be published, 2016.

[3] T. Nakano *et al.*, "Molecular communication and networking: Opportunities and challenges," *IEEE trans. on nanobioscience*, vol. 11, no. 2, pp. 135–148, 2012.

[4] E. Balevi and O. B. Akan, "A physical channel model for nanoscale neuro-spike communications," *IEEE Trans. Commun.*, vol. 61, no. 3, pp. 1178–1187, 2013.

[5] H. Ramezani and O. B. Akan, "Synaptic channel model including effects of spike width variation," in *Proc. of ACM NANOCOM'15*, 2015, p. 11.

[6] D. Malak and O. B. Akan, "A communication theoretical analysis of synaptic multiple-access channel in hippocampal-cortical neurons," *IEEE Trans. commun.*, vol. 61, no. 6, pp. 2457–2467, 2013.

[7] A. Borst and F. E. Theunissen, "Information theory and neural coding." *Nature neuroscience*, vol. 2, no. 11, 1999.

[8] L. Kostal and R. Kobayashi, "Optimal decoding and information transmission in hodgkin–huxley neurons under metabolic cost constraints," *Biosystems*, vol. 136, pp. 3–10, 2015.

[9] A. Manwani and C. Koch, "Detecting and estimating signals over noisy and unreliable synapses: information-theoretic analysis," *Neural computation*, vol. 13, no. 1, pp. 1–33, 2001.

[10] M. Veletić *et al.*, "On the upper bound of the information capacity in neuronal synapses," *IEEE Trans Commun.*, vol. 64, no. 12, pp. 5025–5036, 2016.

[11] L. Galluccio *et al.*, "Characterization of molecular communications among implantable biomedical neuro-inspired nanodevices," *Nano Communication Networks*, vol. 4, no. 2, pp. 53–64, 2013.

[12] H. Ramezani *et al.*, "Rate region analysis of multi-terminal neuronal nanoscale molecular communication channel," in *Proc. of IEEE Nano'17*, 2017.

[13] V. Matveev and X.-J. Wang, "Implications of all-or-none synaptic transmission and short-term depression beyond vesicle depletion: a computational study," *J. Neurosci.*, vol. 20, no. 4, pp. 1575–1588, 2000.

[14] H. Ramezani and O. B. Akan, "Information capacity of vesicle release in neuro-spike communication," *IEEE Communications Letters*, 2017.

[15] D. Mann and P. Yates, "Neurotransmitter deficits in alzheimer's disease and in other dementing disorders." *Human neurobiology*, vol. 5, no. 3, pp. 147–158, 1986.

[16] M. F. Bear *et al.*, *Neuroscience: Exploring the Brain*, 3rd ed. Lippincott Williams & Wilkins, 2007.

[17] J. De La Rocha and N. Parga, "Short-term synaptic depression causes a non-monotonic response to correlated stimuli," *J. Neurosci.*, vol. 25, no. 37, pp. 8416–8431, 2005.

[18] H. Ramezani and O. B. Akan, "Importance of vesicle release stochasticity in neuro-spike communication," in *Proc. of IEEE EMBC'17*, 2017.

[19] V. N. Murthy and C. F. Stevens, "Reversal of synaptic vesicle docking at central synapses," *Nature neuroscience*, vol. 2, pp. 503–507, 1999.

[20] T. Khan *et al.*, "Diffusion-based model for synaptic molecular communication channel," *IEEE Transactions on NanoBioscience*, 2017.

[21] A. Destexhe *et al.*, "kinetic models for synaptic interactions," *The Handbook of Brain Theory and Neural Networks*, pp. 1126–1130, 2002.

[22] M. Fernandez and S. Williams, "Closed-form expression for the poisson-binomial probability density function," *Aerospace and Electronic Systems, IEEE Transactions on*, vol. 46, no. 2, pp. 803–817, April 2010.

[23] L. P. Savtchenko and D. A. Rusakov, "The optimal height of the synaptic cleft," *Proc Natl Acad Sci U S A*, vol. 104, no. 6, pp. 1823–1828, 2007.

[24] T. A. Nielsen *et al.*, "Modulation of glutamate mobility reveals the mechanism underlying slow-rising ampar epscs and the diffusion coefficient in the synaptic cleft," *Neuron*, vol. 42, no. 5, pp. 757–771, 2004.

[25] J. Montes *et al.*, "The influence of synaptic size on ampa receptor activation: A monte carlo model," *PloS one*, vol. 10, no. 6, p. e0130924, 2015.

[26] N. Agmon and A. L. Edelstein, "Collective binding properties of receptor arrays." *Biophys. J.*, vol. 72, no. 4, p. 1582, 1997.

[27] L. E. Dobrunz and C. F. Stevens, "Heterogeneity of release probability, facilitation, and depletion at central synapses," *Neuron*, vol. 18, no. 6, pp. 995–1008, 1997.

[28] T. Schikorski and C. F. Stevens, "Quantitative ultrastructural analysis of hippocampal excitatory synapses," *J. Neurosci.*, vol. 17, no. 15, pp. 5858–5867, 1997.

[29] D. A. Rusakov *et al.*, "Shaping the synaptic signal: molecular mobility inside and outside the cleft," *Trends in neurosciences*, vol. 34, no. 7, pp. 359–369, 2011.

[30] F. Ventriglia and V. Di Maio, "A brownian simulation model of glutamate synaptic diffusion in the femtosecond time scale," *Biological cybernetics*, vol. 83, no. 2, pp. 93–109, 2000.